



| | |
|------------------|---|
| Title | Intense winter cooling of the surface water in the northern Okinawa Trough during the last glacial period |
| Author(s) | Yamamoto, Masanobu; Kishizaki, Midori; Oba, Tadamichi; Kawahata, Hodaka |
| Citation | Journal of Asian Earth Sciences, 69, 86-92 https://doi.org/10.1016/j.jseaes.2012.06.011 |
| Issue Date | 2013-06-05 |
| Doc URL | http://hdl.handle.net/2115/53019 |
| Type | article (author version) |
| File Information | HUSCAP_yamamoto.pdf |



[Instructions for use](#)

1 **Intense winter cooling of the surface water in the northern Okinawa**
2 **Trough during the last glacial period**

3
4 Masanobu Yamamoto^{1,*}, Midori Kishizaki¹, Tadamichi Oba¹, Hodaka Kawahata²

5
6 ¹Faculty of Environmental Earth Science, Hokkaido University, Sapporo, Japan

7 ²Atmosphere and Ocean Research Institute, The University of Tokyo, Kashiwa, Chiba,
8 Japan

9 *Corresponding author: Tel.: +81-11-706-2379; fax: +81-11-706-4867

10 E-mail address: myama@ees.hokudai.ac.jp (M. Yamamoto)

11 Key words: thermocline temperature, TEX₈₆, MD98-2195, the East China Sea, Okinawa
12 Trough, LGM, winter monsoon

13
14 **Abstract**

15 We generated a 42,000-year record of TEX₈₆ (TEX₈₆^L and TEX₈₆^H) from core MD98-2195
16 to better understand changes in the hydrology of the East China Sea (ECS) in the last glacial
17 period. The TEX₈₆-derived temperature showed an intense cooling in the last glacial period,
18 whereas U₃₇^{K'}-derived spring sea surface temperature (SST) and foraminiferal Mg/Ca-derived
19 summer SST showed a much smaller-scale cooling. The difference between the TEX₈₆- and
20 Mg/Ca-derived temperatures was around 14°C from 19 to 16 ka and abruptly decreased to
21 around 5°C from 16 to 13 ka. This suggests a strong winter cooling of the surface water
22 during the last glacial period. TEX₈₆-, U₃₇^{K'}-, and Mg/Ca-derived temperatures were lowest at
23 18 to 17 ka, implying that the formation of cold water was maximized during that period.
24 These results show that the cold water mass developed in the northern Okinawa Trough
25 during the last glacial and the Kuroshio branch did not fully enter the northern margin of the

26 Okinawa Trough.

27

28 Key words: temperature, TEX₈₆, MD98-2195, the East China Sea, the last glacial period

29

30 **1. Introduction**

31 The East China Sea (ECS) is a marginal sea bounded by the Asian continent on its west, the
32 island of Taiwan on its southwest, the Ryukyu Islands on its southeast, and Kyushu and the
33 Korean Peninsula on its northeast and north, respectively (Fig. 1a). The hydrological
34 evolution of the ECS and the surrounding areas since the last glacial period has been
35 investigated using assemblages, $\delta^{18}\text{O}$, $\delta^{13}\text{C}$ and Mg/Ca data from planktonic foraminifera (e.g.,
36 Ujiie et al., 1991, 2003; Jian et al., 1996, 2000; Li et al., 1997; Shieh et al., 1997; Ujiie and
37 Ujiie, 1999, 2006; Xu and Oda, 1999; Li et al., 2001; Ijiri et al., 2005; Sun et al., 2005; Lin et
38 al., 2006; Chang et al., 2008; Chen et al., 2010; Kubota et al., 2010), U_{37}^{K} (e.g., Meng et al.,
39 2002; Ijiri et al., 2005; Zhao et al., 2005; Zhou et al., 2007; Yu et al., 2008; Li et al., 2009;
40 Wang et al., 2011), nannofossil assemblages (Ujiie et al., 1991; Ahagon et al., 1993), bulk
41 biogenic, sulfur and lithogenic contents (Wahyudi and Minagawa, 1997; Kao et al., 2006a;
42 Chang et al., 2009), mineralogy (Chen et al., 2011), the $\delta^{13}\text{C}$ of benthic foraminifera
43 (Wahyudi and Minagawa, 1997), and pollen from marine cores (Kawahata and Ohshima,
44 2004), and modeling (Kao et al., 2006b). The ECS is characterized by a large environmental
45 contrast between the Holocene and the last glacial period. On the basis of nannofossil and
46 planktonic foraminifera assemblages (Ujiie et al., 1991; Ahagon et al., 1993; Ujiie and Ujiie,
47 1999; Ujiie et al., 2003), it was suggested that the Kuroshio did not flow into the ECS because
48 of a blockage caused by a topographic barrier between Taiwan and Yonaguni Island. In
49 contrast, other studies have assumed that the inflow of the Kuroshio continued during the last
50 glacial period (e.g., Xu and Oda, 1999; Kawahata and Ohshima, 2004; Ijiri et al., 2005; Sun et
51 al., 2005; Kao et al., 2006b; Chen et al., 2010). The difference in SST between the last glacial

52 maximum (LGM) and the late Holocene was estimated to be 1 to 3°C in the central Okinawa
53 Trough (Li et al., 2001; Sun et al., 2005; Zhao et al., 2005; Zhou et al., 2007; Chang et al.,
54 2008; Chen et al., 2010) and 4 to 6°C in the northern Okinawa Trough (Xu and Oda, 1999;
55 Ijiri et al., 2005; Kubota et al., 2010). The northern Okinawa Trough was more sensitive to
56 climate changes than the central Okinawa Trough.

57 Xu and Oda (1999) discussed environmental changes in the northern Okinawa Trough
58 during the last 36 kyr based on planktonic foraminiferan assemblages and oxygen isotopes of
59 *Globigerina bulloides*. They recognized a period influenced by coastal water from 36 to 19.5
60 ka, a period influenced by coastal water and extremely low salinity from 19.5 to 10.5 ka, and
61 a period of both high temperatures and high salinity after 10.5 ka controlled by modern open
62 sea water related to the Kuroshio. Ijiri et al. (2005) further discussed changes in the northern
63 Okinawa Trough hydrological conditions based on planktonic foraminiferan assemblages, the
64 oxygen-carbon isotopes of *Globigerinoides ruber*, and $U_{37}^{K'}$. They recognized a strong
65 upwelling period from 42 to 24 ka, a period of cold and less saline water mass from 24 to 14
66 ka, a transitional period from cold to warm water masses from 14 to 8 ka, and the present-day
67 warm Kuroshio condition after 8 ka. Both studies hypothesized that the Kuroshio entered in
68 the Okinawa Trough but weakened during the LGM and the early stages of the last
69 deglaciation in response to the expansion of the coastal water in the northern Okinawa
70 Trough. It is, however, not clear what forcing caused the expansion of the coastal water.

71 In this study, we generated a record of TEX₈₆-derived temperatures from the core
72 MD98-2195 taken in the northern Okinawa Trough during the last 42 ky to better understand
73 the hydrology of the northern Okinawa Trough in the last glacial period (Fig. 1a). These data,
74 together with published data of $U_{37}^{K'}$ -derived SST from the same core (Ijiri et al., 2005) and
75 planktonic foraminiferan Mg/Ca-derived SST data from the nearby KY07-04 PC-1 core
76 (Kubota et al., 2010), provide surface and subsurface temperature records for the last 42 kyr
77 that can be used to assess changes in the hydrology of the northern Okinawa Trough.

78 Although the Holocene record of TEX₈₆ at a nearby site is reported by Nakanishi et al.
79 (submitted to Journal of Quaternary Science), this is the first report of the TEX₈₆ record that
80 extends to the last glacial period in the ECS

81

82 **2. Modern oceanography of the study site**

83 Today, the hydrology of the ECS is affected by changes in the strength of the Kuroshio and
84 the East Asian monsoon. The Kuroshio is a western boundary current in the western North
85 Pacific Ocean that transports warm, saline water northward and forms temperature and
86 salinity gradients by mixing with cool, less saline water in the ECS (Ichikawa and Beardsley,
87 2002). Summer monsoon precipitation over south and central China provides freshwater
88 discharge to the ECS, where a less saline surface layer develops. Winter monsoon winds cool
89 and mix the water in the Yellow Sea (YS) and the western ECS, forming cold bottom water
90 on the continental shelf in the ECS and YS (Uda, 1934; Ichikawa and Beardsley, 2002; Zhang
91 et al., 2008). Under intense winter cooling, the YS and the ECS are well mixed in the upper
92 100 m. Because the thermal inertia of a water column on the shelf is linearly proportional to
93 the bottom depth, which determines the cooling rate of the water column, the winter SST is
94 lower in the shallower shelf than in the deeper shelf (Xie et al., 2002).

95 At the study site, warm, saline Kuroshio water meets the less saline Changjiang Diluted
96 Water (CDW)/Yellow Sea Central Cold Water (YSCCW). The Kuroshio carries warm and
97 saline water along the Ryukyu Islands. There is a clear boundary between the shelf water and
98 warm Kuroshio water in winter (Fig. 1b). Temperature and salinity are nearly constant from
99 surface to 100 meters depth at the study site. In summer, less-saline water originating from
100 the CDW mixes with the sea-surface water, and a thermocline develops mainly due to
101 radiative heating by insolation. As a result, the spatial temperature variation is small at the
102 surface. At 50-m depth, the cold and less saline YSCCW spreads over the continental shelf.
103 This water mass is formed in the YS in winter cooling, reaches to the northern Okinawa

104 Trough by southeastward advection and continues to exist from spring to fall (Uda, 1934;
105 Ichikawa and Beardsley, 2002; Zhang et al., 2008).

106 The maximum SST near the core site is 28.3°C in August, and the minimum is 17.5°C in
107 February (Fig. 2b; Japan Oceanographic Data Center; <http://www.jodc.go.jp/index.html>). SSS
108 reaches a maximum value of 34.7 (practical salinity scale) in February and a minimum value
109 of 33.2 in July when discharge from the Changjiang (Yangtze River) peaks.

110

111 **3. Samples and methods**

112 *3.1. Study cores and age-depth model*

113 During the IMAGES IV cruise in 1998, a 33.65-m-long giant piston core (MD98-2195)
114 was collected from a water depth of 746 m on the northern slope of the Okinawa Trough at
115 31°38.33'N, 128°56.63'E (Fig. 1a). The sediment of MD98-2195 consists of olive-colored
116 silty clay with sandy intervals at 15.28 to 15.30 m depth (Ijiri et al., 2005). Two ash layers,
117 Kikai-Akahoya (K-Ah) and Aira-Tanzawa (AT), are intercalated at depths of 5.1 to 6.0 m and
118 21.8 to 22.9 m, respectively.

119 An age model in calendar years (Fig. 3; Ijiri et al., 2005) was created from the AMS ¹⁴C
120 ages of fourteen samples of the planktonic foraminifera *Neogloboquadrina dutertrei* and/or
121 *Globigerina bulloides* and two ash layers: K-Ah (7.3 ka; Kitagawa et al., 1995) and AT (25.9
122 ka; Kitagawa and van der Plicht, 1998). The calendar age was converted using the CALIB5.0
123 program and dataset Marine04 (Hughen et al., 2004), with local corrections for a
124 surface-ocean reservoir age (delta-R) of 0 years.

125 A total of 71 samples were collected from core MD98-2195 between the core top and a
126 depth of 33.63 m (0–42.0 ka).

127

128 *3.2. Analytical methods*

129 Glycerol dialkyl glycerol tetraethers (GDGTs) were analyzed following Yamamoto and

130 Polyak (2008). Lipids were extracted (3 x) from a freeze-dried sample using a DIONEX
131 Accelerated Solvent Extractor ASE-200 at 100°C and 1000 psi for 10 min with 11 ml of
132 CH₂Cl₂/CH₃OH (6:4) and then concentrated. The extract was separated into four fractions
133 using column chromatography (SiO₂ with 5% distilled water; i.d., 5.5 mm; length, 45 mm): F1
134 (hydrocarbons), 3ml hexane; F2 (aromatic hydrocarbons), 3 ml hexane–toluene (3:1); F3
135 (ketones), 4 ml toluene; F4 (polar compounds), 3 ml toluene–CH₃OH (3:1). An aliquot of F4
136 was dissolved in hexane-2-propanol (99:1) and filtered.

137 GDGTs in F4 were analyzed using high performance liquid chromatography-mass
138 spectrometer (HPLC-MS) with an Agilent 1100 HPLC system connected to a Bruker
139 Daltonics micrOTOF-HS time-of-flight mass spectrometer. Separation was conducted using a
140 Prevail Cyano column (2.1 x 150 mm, 3µm; Alltech) maintained at 30°C following the method
141 of Hopmans et al. (2000) and Schouten et al. (2007). Conditions were: flow rate 0.2 ml/min,
142 isocratic with 99% hexane and 1% 2-propanol for the first 5 min followed by a linear gradient
143 to 1.8% 2-propanol over 45 min. Detection was achieved using atmospheric pressure, positive
144 ion chemical ionization-MS (APCI-MS). The spectrometer was run in full scan mode (*m/z*
145 500–1500). Compounds were identified by comparing mass spectra and retention times with
146 those of GDGT standards (obtained from the main phospholipids of *Thermoplasma*
147 *acidophilum* via acid hydrolysis) and those in the literature (Hopmans et al., 2000).
148 Quantification was achieved by integrating the summed peak areas in the (M+H)⁺ and the
149 isotopic (M+H+1)⁺ chromatograms. TEX₈₆ and TEX₈₆^H (applicable to warm water) were
150 calculated from the concentrations of GDGT-1, GDGT-2, GDGT-3 and a regioisomer of
151 crenarchaeol using the following expressions (Schouten et al., 2002; Kim et al., 2010):

152

$$153 \quad \text{TEX}_{86} = ([\text{GDGT-2}] + [\text{GDGT-3}] + [\text{Crenarchaeol regioisomer}]) /$$

$$154 \quad ([\text{GDGT-1}] + [\text{GDGT-2}] + [\text{GDGT-3}] + [\text{Crenarchaeol regioisomer}])$$

$$155 \quad \text{TEX}_{86}^{\text{H}} = \log (\text{TEX}_{86})$$

156

157 TEX_{86}^L , applicable in cooler water, was calculated from the concentrations of GDGT-1,
158 GDGT-2 and GDGT-3 using the following expression (Kim et al., 2010):

159

$$160 \quad \text{TEX}_{86}^L = \log \{ [\text{GDGT-2}] / ([\text{GDGT-1}] + [\text{GDGT-2}] + [\text{GDGT-3}]) \}$$

161

162 Temperature was calculated according to the following equation based on a global core top
163 calibration (Kim et al., 2010):

164

$$165 \quad T = 68.4\text{TEX}_{86}^H + 38.6 \text{ (when } T > 15^\circ\text{C)}$$

$$166 \quad T = 67.5\text{TEX}_{86}^L + 46.9 \text{ (when } T < 15^\circ\text{C)}$$

167

168 where T = temperature [$^\circ\text{C}$]; The standard errors averaged 0.7°C .

169

170 **4. Results**

171 The temperatures calculated from TEX_{86}^H were a maximum of 3°C lower than those from
172 TEX_{86}^L (Fig. 4). Kim et al. (2010) recommended that TEX_{86}^H , which includes the abundance
173 of crenarchaeol regio-isomer, be used in tropical and subtropical regions ($>15^\circ\text{C}$) and that
174 TEX_{86}^L , which excludes the abundance of crenarchaeol regio-isomer, be used in polar and
175 subpolar regions ($<15^\circ\text{C}$) because crenarchaeol regio-isomer plays a more important role for
176 temperature adaptation in subtropical than in subpolar oceans. Because TEX_{86}^L - and TEX_{86}^L
177 -derived temperatures exceeded 15°C at 11.5 ka, we use TEX_{86}^L from 42 ka to 11.5 ka and
178 TEX_{86}^H after 11.5 ka for further discussion in this study.

179 The TEX_{86} -derived temperature fluctuated around 15°C from 42 to 27 ka, decreased to 9°C
180 from 27 to 18 ka, increased to 18°C from 18 to 13 ka, and gradually increased to 22°C from

181 13 ka to the present (Fig. 4). The $\text{TEX}_{86}^{\text{H}}$ - and $\text{TEX}_{86}^{\text{L}}$ -based temperatures at the core-top
182 sample (surface sediment, 0–1 cm) of core PL-1 are 22.6°C and 22.8°C, respectively. These
183 temperatures agreed with mean annual SST (22.4°C; Japan Oceanographic Data Center;
184 available at <http://www.jodc.go.jp/index.html>), the SSTs in May and November or the
185 temperature from June to November at depths of 50–70 m (Fig. 2).

186 Branched and isoprenoid tetraether (BIT) index values (Hopmans et al., 2004) ranged from
187 0.001 to 0.005 in the samples analyzed (Fig. 5), indicating a low contribution of terrestrial
188 soil organic matter at the study site over the last 42 kyr. Weijers et al. (2006) noted that
189 samples with high BIT values (> 0.4) may show anomalously high TEX_{86} -derived
190 temperatures. This concern is, however, not relevant for the samples used in this study. BIT
191 values showed double maxima at 39 ka and 15 ka (Fig. 5), indicating an enhanced input of
192 soil organic matter.

193

194 **5. Discussion**

195 **5.1. Glacial–interglacial contrast in water temperature**

196 The temperatures estimated using TEX_{86} differed from those obtained using $U_{37}^{\text{K}'}$ from the
197 study core (Ijiri et al., 2005) and the Mg/Ca ratio of the planktonic foraminifera
198 *Globigerinoides ruber* from the nearby KY07-04 PC-1 core (Kubota et al., 2010) (Fig. 4).
199 The TEX_{86} -derived temperatures were approximately 21°C ($\text{TEX}_{86}^{\text{H}}$) in the late Holocene and
200 13°C ($\text{TEX}_{86}^{\text{L}}$) in the LGM, a 8°C difference (Fig. 4). In contrast, the Mg/Ca-derived
201 temperatures were 26°C in the late Holocene and 22°C in the early deglaciation, a 4°C
202 difference, and the $U_{37}^{\text{K}'}$ -derived temperatures were 24°C in the late Holocene and 21°C in the
203 LGM, a 3°C difference (Fig. 4).

204 The Mg/Ca-derived temperature is assumed to indicate SST from May to August, based on
205 the core-top value (Kubota et al., 2010) and seasonal variation in the sinking flux (Xu et al.,
206 2005). The $U_{37}^{\text{K}'}$ -derived temperature for the core-top sample of core PL-1 is 22.3°C. This

207 temperature is similar to the mean annual SST (22.4°C; Japan Oceanographic Data Center;
208 available at <http://www.jodc.go.jp/index.html>) and the SST in May and November at this site
209 (Fig. 2). Analysis for particulate organic matter in May showed a maximal concentration of
210 alkenones between depths of 5 and 20 m, and the $U_{37}^{K'}$ values were consistent with the in situ
211 water temperature (Nakanishi et al., submitted to Journal of Oceanography). A one-year
212 time-series sediment trap experiment indicated that the sinking flux of *Emiliania huxleyi* was
213 maximal from March to May (Tanaka et al., 2003). These observations suggest that the $U_{37}^{K'}$
214 reflects the SST in spring.

215 The season and depth of GDGT production in the ECS are not clear. The TEX_{86}^H - and
216 TEX_{86}^L -based temperatures (22.6°C and 22.8°C, respectively) at the core-top sample of core
217 PL-1 agreed with mean annual SST, the SSTs in May and November, and the temperature
218 from June to November at depths of 50–70 m (Fig. 2) TEX_{86} is less likely to reflect the SST in
219 a specific short period such as May or November for the following two reasons. First, analysis
220 of GDGTs in particulate organic matter sampled during the spring bloom in May 2008 in the
221 study area (Nakanishi et al., submitted) showed a low GDGT concentration and lower
222 TEX_{86} -derived temperature than in situ temperature in the surface water column (< 20m),
223 suggesting that TEX_{86} did not reflect the SST in May at the study site. Second, a
224 sediment-trap study in the western North Pacific showed nearly constant TEX_{86} values in
225 sinking particles, roughly corresponding to the mean annual SST throughout the entire year,
226 although there was a large seasonal variation in SST, implying that GDGTs produced in
227 different seasons were suspended and well mixed in the surface water (Yamamoto et al.,
228 2012). These observations suggest that TEX_{86} reflects the average temperature in multiple
229 seasons rather than the temperature in a specific time interval. This property is different from
230 that of $U_{37}^{K'}$ and foraminiferal Mg/Ca, which reflects the temperature in the bloom and
231 growing period (spring, and spring to summer in the ECS, respectively). Thus, the most likely
232 interpretation is that TEX_{86} reflects either mean annual SST or summer subsurface water

233 temperature. Although TEX_{86} is usually thought to reflect SST (Schouten et al., 2002; Kim et
234 al., 2008; 2010), a sediment-trap study in the Santa Barbara Basin found that TEX_{86} reflected
235 subsurface rather than surface temperatures (Huguet et al., 2006b). The TEX_{86} in tropical
236 North Atlantic sediments was also assumed to reflect subsurface water temperature (Lopes
237 dos Santos et al., 2010). Analysis of particulate organic matter collected in May 2008 in the
238 northern Okinawa Trough showed a broad peak in GDGT concentrations at depths between
239 50 and 100 m and TEX_{86} values consistent with local water temperature at those depths,
240 which suggests in situ production of GDGTs in the 50–100 m depth interval (Nakanishi et al.,
241 submitted). This observation indicates possible production of GDGTs in the thermocline.
242 TEX_{86} -derived temperatures from surface sediments from the southern ECS were 0–2°C
243 lower than mean annual SSTs (Zhu et al., 2011), whereas those from the YS and the northern
244 SCS were much lower than the mean annual SSTs and corresponded to winter SSTs or
245 subsurface water temperatures (Kyun-Hoon Shin, unpublished data). Therefore, the
246 possibility that TEX_{86} reflects thermocline temperature cannot be ignored in the ECS.

247 Although it is not clear whether TEX_{86} reflects the mean annual SST or the summer
248 thermocline temperature, interpretation of TEX_{86} variation is possible because both
249 temperatures are determined by a common forcing, as discussed below. The site of this study
250 is located east of the contact zone between the YSCCW/CDW and the KWS, and the
251 southward migration of the YSCCW was detected by hydrographical measurements at the
252 station west of Jeju Island (Zhang et al., 2008). A steep temperature gradient in the northern
253 Okinawa Trough suggests the influence of the YACCW/CDW at the study site (Fig. 1b and
254 c). In the modern summer at a depth of 50 m, the cold and relatively less saline YSCCW
255 spreads over the continental shelf of the YS and the ECS (Fig. 1b). This water mass forms in
256 the YS as a result of winter cooling and reaches the northern Okinawa Trough by advection,
257 where it exists from spring until fall (Ichikawa and Beardsley, 2002; Zhang et al., 2008).
258 Because the summer thermocline temperature is linked to winter SST, it is also a consequence

259 of winter cooling. Although it is not clear whether TEX_{86} reflects the mean annual SST or the
260 summer thermocline temperature, TEX_{86} likely responds to the surface cooling of the YS
261 and/or the ECS by the East Asian winter monsoon.

262 The difference between the TEX_{86} - and Mg/Ca-derived temperatures was around 14°C
263 from 19 to 16 ka and abruptly decreased to around 5°C from 16 to 13 ka (Fig. 4). In the case
264 that TEX_{86} reflects the summer thermocline temperature, this change suggests that the
265 summer thermocline was more developed in the last glacial period than in the Holocene. A
266 steep gradient between surface and subsurface temperatures (24°C at 5 m, and 7°C at 50 m in
267 in July in the northern YS; Zhang et al., 2008) is currently observed in the YS in the summer.
268 In the case that TEX_{86} reflects SST, it is suggested that the seasonal difference in SST was
269 larger in the last glacial period than in the Holocene. A large seasonal SST difference (ca.
270 18°C at 5 m depth in the northern YS; Zhang et al., 2008) is currently observed in the YS as
271 well. The modern YS is a potential analog of the northern Okinawa Trough in the LGM.

272 In the last glacial period, the continental shelf of the present ECS was largely exposed due
273 to a low sea level stand (maximum 130 m), and the study site was located near the continent
274 (Fig. 6). Because the thermal inertia of a water column on the shelf is linearly proportional to
275 the bottom depth (Xie et al., 2002), winter monsoon winds could have efficiently formed a
276 cold water mass near the study site in the LGM, whereas the surface water would have been
277 warmed by insolation and by heat exchange with the atmosphere during spring and summer.
278 The northern Okinawa Trough was hydrologically characterized by a strong cooling of the
279 surface water during the winter and a well-developed halocline during the summer (Xu and
280 Oda, 1999; Ijiri et al., 2005). This resulted in the large difference between Mg/Ca-derived and
281 TEX_{86} -derived temperatures in the northern Okinawa Trough.

282

283 **5.2. Temperature changes during the last deglaciation**

284 TEX_{86} , U_{37}^{K} , and planktonic foraminiferal Mg/Ca data showed similar variation in

285 estimated temperature for the study site (Fig. 4), despite differences in the amplitudes of
286 variation. The temperatures gradually decreased from 42 to 18 ka, were lowest at 18 to 17 ka,
287 and abruptly increased from 17 to 13 ka, centered at 14.5 ka (Fig. 4). This pattern was also
288 common in the central Okinawa Trough (Li et al., 2001; Zhao et al., 2005; Sun et al., 2005;
289 Zhou et al., 2007; Chang et al., 2008; Chen et al., 2010). At the study site, winter SST and the
290 summer temperature at the thermocline are governed by the mixing of the cold shelf water
291 (CDW and/or YSCCW) and Kuroshio water. Decreased TEX_{86} at 17–18 ka is thus
292 attributable either to the intensification of the Kuroshio or to shrinkage of the CDW and the
293 YSCCW. A weakening of the Kuroshio jet during the last deglaciation was suggested based
294 on a SST record from offshore central Japan (Yamamoto et al., 2005; Yamamoto, 2009). This
295 correspondence suggests that the weakening of the Kuroshio is the first possible factor
296 affecting the TEX_{86} in the northern Okinawa Trough.

297 In addition, a similar pattern was observed in the TEX_{86} record from the northern South
298 China Sea (Shintani et al., 2011). The paleotemperature difference between the northern
299 South China Sea and the Sulu Sea suggested that the East Asian winter monsoon gradually
300 intensified after 21 ka, maximized at 12 ka, and weakened toward the late Holocene (Shintani
301 et al., 2008). The paleotemperature gradient between the western and eastern margins of the
302 South China Sea suggested that the East Asian winter monsoon gradually intensified after 21
303 ka, maximized during the Oldest Dryas and Younger Dryas periods, and weakened towards
304 the late Holocene (Huang et al., 2011). Changes in the TEX_{86} -derived temperatures at the
305 study site are roughly consistent with changes in the East Asian winter monsoon inferred
306 from paleotemperature records from the South China Sea. Because the South China Sea does
307 not suffer a direct influence of Kuroshio variation, the intensity of the East Asian winter
308 monsoon is the second factor affecting TEX_{86} in the study site.

309 In contrast to the South China Sea, the TEX_{86} record from the study site did not show a
310 significant cooling in the Younger Dryas period. The formation of cold water in winter is

311 generally more active in shallow shelf areas than in deeper areas. The source area of the
312 cooled water shifted westward far from the study site due to marine transgression during the
313 Younger Dryas period and the TEX₈₆-derived temperature became insensitive to changes in
314 the intensity of the East Asian winter monsoon. The Younger Dryas cooling thus did not
315 decrease TEX₈₆ significantly in the study site. The formation of cold water gradually
316 intensified from 42 to 18 ka due to both a low sea level stand and a stronger winter monsoon,
317 maximized at 18 to 17 ka, abruptly weakened from 17 to 13 ka due to a marine transgression,
318 and then gradually weakened afterwards. Therefore, we suggest that the formation of cold
319 water in the northern Okinawa Trough was regulated by a combination of the intensity of the
320 Kuroshio, the intensity of the East Asian winter monsoon and the proximity of the coast.

321

322 **5.3. Oceanographic linkage with the Sea of Japan**

323 The northern Okinawa Trough is the source region of the Tsushima Warm Current that
324 flows in the Sea of Japan (Fig. 1b and c). The Sea of Japan was semi-isolated, well stratified
325 and anoxic from 24 to 18 ka, resulting in the deposition of a thick dark layer (Oba et al.,
326 1991; Tada et al., 1999). Oba et al. (1991) suggested that Huanghe (Yellow River) flowed
327 into the Sea of Japan, forming less saline surface water. Tada et al. (1999) assumed that the
328 freshwater inputs of the Changjiang and Huanghe rivers formed less saline water in the
329 paleo-ECS that flowed into the Sea of Japan.

330 Today, the Kuroshio branch current west of Kyushu (KBCWK) passes through the western
331 flank of the northern Okinawa Trough (Fig. 1b and c; Ichikawa and Beardsley, 2002) and
332 becomes the Tsushima Warm Current by mixing with the ECS water. Xu and Oda (1999)
333 demonstrated that the less saline and low temperature species *Globigerina quinqueloba*
334 frequently occurred from 19.5 to 10.5 ka in the northern Okinawa Trough. Ijiri et al. (2005)
335 subsequently showed the presence of a cold and less saline water mass in the northern
336 Okinawa Trough from 24 to 14 ka, based on high abundance of *Neogloboquadrina*
337 *pachyderma*, *Neogloboquadrina incompta*, and *Globigerina quinqueloba*. They further

338 indicated the freshwater influence on the surface water during this period based on the $\delta^{18}\text{O}$
339 of planktonic foraminifera. Our study demonstrates the development of a cold water mass in
340 the northern Okinawa Trough during the LGM (Fig. 6). These results suggest that the
341 KBCWK did not fully enter the northern Okinawa Trough. Because the KBCWK weakened,
342 the inflow of saline water into the Sea of Japan decreased, resulting in the development of a
343 halocline in the Sea of Japan during the LGM.

344

345 **6. Conclusions**

346 The TEX_{86} -derived temperature showed intense cooling in the last glacial period, whereas
347 $U_{37}^{\text{K}'}$ -derived spring sea surface temperature (SST) and Mg/Ca-derived summer SST showed
348 much smaller-scale cooling. In the last glacial period, the hydrology of the northern Okinawa
349 Trough was characterized by strong cooling of the surface water in winter and the
350 development of cold subsurface water during summer.

351 TEX_{86} -, $U_{37}^{\text{K}'}$ -, and planktonic foraminiferal Mg/Ca-derived temperatures gradually
352 decreased from 42 to 18 ka, were lowest at 18 to 17 ka, abruptly increased from 17 to 13 ka
353 centered at 14.5 ka, reflecting changes in cold water formation in the northern Okinawa
354 Trough

355 During the LGM, the development of a cold-water mass in the northern Okinawa Trough
356 could have prevented the saline Kuroshio water from flowing into the northern Okinawa
357 Trough and the Sea of Japan, resulting in the development of a halocline in the Sea of Japan
358 during the LGM.

359

360 **Acknowledgements.** We thank late Luejiang Wang (Hokkaido University) for providing
361 MD98-2195 samples. Thanks also go to Tatsufumi Okino, Masao Minagawa, Noriko
362 Edasawa, Keiko Ohnishi, and Youichi Tanimoto (Hokkaido University) for help with analysis
363 and discussion. Akira Ijiri (JAMSTEC) and Yoshimi Kubota (University of Tokyo) kindly
364 provided the electric data of the $U_{37}^{\text{K}'}$ in MD98-2195 core and the Mg/Ca ratio in LY07-04

365 PC-1 core, respectively. We also thank Min-Te Chen and two anonymous reviewers for their
366 constructive comments. We appreciate Prof. Chi-Yue Huang for his contributions to the
367 studies on East China Sea paleoceanography. This study was supported by a grant-in-aid for
368 Scientific Research (A) the Japan Society for the Promotion of Science, No. 19204051 (to
369 MY).

370

371 **References**

372 Ahagon, N., Tanaka, Y., Ujiie, H., 1993. *Florisphaera profunda*, a possible nanoplankton
373 indicator of late Quaternary changes in sea-surface turbidity at the northern margin of the
374 Pacific. *Marine Micropaleontology* 22, 255–273.

375 Chang, Y.-P., Wang, W.-L., Yokoyama, Y., Matsuzaki, H., Kawahata, H., Chen, M.T., 2008.
376 Millennial-scale planktic foraminifer faunal variability in the East China Sea during the
377 past 40000 years (IMAGES MD012404 from the Okinawa Trough). *Terrestrial,
378 Atmospheric and Oceanic Sciences* 19, 389–401.

379 Chang, Y.-P., Chen, M.-T., Yokoyama, Y., Matsuzaki, H., Thompson, W.G., Kao, S.J.,
380 Kawahata, H., 2009. Monsoon hydrography and productivity changes in the East China
381 Sea during the past 100,000 years: Okinawa Trough evidence (MD012404).
382 *Paleoceanography* 24, PA3208.

383 Chen, M.-T., Lin, X.P., Chang, Y.-P., Chen, Y.-C., Lo, L., Shen, C.-C., Yokoyama, Y., Oppo,
384 D.W., Thompson, W.G., Zhang, R., 2010. Dynamic millennial-scale climate changes in the
385 northwestern Pacific over the past 40,000 years. *Geophysical Research Letters* 37, L23603.

386 Chen, H.F., Chang, Y.P., Kao, S.J., Chen, M.T., Song, S.R., Luo, L.W., Wen, S.Y., Yang,
387 T.N., Lee, T.Q., 2011. Mineralogical and geochemical investigations of sediment-source
388 region changes in the Okinawa Trough during the past 100 ka (IMAGES core MD012404):
389 *Journal of Asian Earth Sciences* 40, 1238-1249.

390 Hopmans, E.C., Schouten, S., Pancost, R., van der Meer, M.T.J., Sinninghe Damsté, J.S., 2000.

391 Analysis of intact tetraether lipids in archaeal cell material and sediments by high
392 performance liquid chromatography/atmospheric pressure chemical ionization mass
393 spectrometry. *Rapid Communications in Mass Spectrometry* 14, 585–589.

394 Hopmans, E.C., Weijers, J.W.H., Schefuss, E., Herfort, L., Sinninghe Damsté, J.S., Schouten,
395 S., 2004. A novel proxy for terrestrial organic matter in sediments based on branched and
396 isoprenoid tetraether lipids. *Earth and Planetary Science Letters* 224, 107–116.

397 Huang, E., Tian, J., Steinke, S., 2011. Millennial-scale dynamics of the winter cold tongue in
398 the southern South China Sea over the past 26 ka and the East Asian winter monsoon.
399 *Quaternary Research* 75, 196–204.

400 Hughen, K.A., Baillie, M.G.L., Bard, E., Beck, J.W., Bertrand, C.J.H., Blackwell, P.G., Buck,
401 C.E., Burr, G.S., Cutler, K.B., Damon, P.E., Edwards, R.L., Fairbanks, R.G., Friedrich, M.,
402 Guilderson, T.P., Kromer, B., McCormac, G., Manning, S., Ramsey, C.B., Reimer, P.J.,
403 Reimer, R.W., Remmele, S., Southon, J.R., Stuiver, M., Talamo, S., Taylor, F.W., van der
404 Plicht, J., Weyhenmeyer, C.E., 2004. MARINE04 marine radiocarbon age calibration, 0 –
405 26 cal kyr BP. *Radiocarbon* 46, 1059–1086.

406 Huguet, C., Kim, J.-H., Sinninghe Damsté, J.S., Schouten, S., 2006. Reconstruction of sea
407 surface temperature variations in the Arabian Sea over the last 23 kyr using organic proxies
408 (TEX₈₆ and U₃₇^{K'}). *Paleoceanography* 21, PA300S.

409 Ichikawa, H., Beardsley, R.C., 2002. The current system in the Yellow and East China Seas.
410 *Journal of Oceanography* 58, 77–92.

411 Ijiri, A., Wang, L., Oba, T., Kawahata, H., Huang, C.Y., Huang, C.Y., 2005.
412 Paleoenvironmental changes in the northern area of the East China Sea during the past
413 42,000 years. *Palaeogeography, Palaeoclimatology, Palaeoecology* 219, 239–261.

414 Japan Oceanographic Data Center (JODC) 1906–2003. Oceanographic data, monthly
415 sea-surface temperature in the East China Sea, <http://www.jodc.go.jp/index.html>, Japan
416 Hydrographic Association, Tokyo, Japan.

417 Jian, Z., Li, B., Pflaumann, U., Wang, P., 1996. Late Holocene cooling event in the western
418 Pacific. *Science in China (Series D)* 39, 543–550.

419 Jian, Z.S., Wang, P.X., Saito, Y., Wang, L.J., Pflaumann, U., Oba, T., Cheng, X.R., 2000.
420 Holocene variability of the Kuroshio Current in the Okinawa Trough, northwestern Pacific
421 Ocean. *Earth and Planetary Science Letters* 184, 305–319.

422 Kao, S.J., Roberts, A.P., Hsu, S.C., Chang, Y.P., Lyons, W.B., Chen, M.-T., 2006a. Monsoon
423 forcing, hydrodynamics of the Kuroshio Current, and tectonic effects on sedimentary
424 carbon and sulfur cycling in the Okinawa Trough since 90 ka. *Geophysical Research*
425 *Letters* 33, L05610.

426 Kao, S.J., Wu, C.R., Hsin, Y.C., Dai, M., 2006b. Effects of sea level changes on the upstream
427 Kuroshio Current through the Okinawa Trough. *Geophysical Research Letters* 33, L16604.

428 Kawahata, H., Ohshima, H., 2004. Vegetation and environmental record in the northern East
429 China Sea during the late Pliocene. *Global and Planetary Change* 41, 251–273.

430 Kim, J.H., van der Meer, J., Schouten, S., Helmke, P., Willmott, V., Sangiorgi, F., Koc, N.,
431 Hopmans, E.C., Sinninghe Damsté, J.S., 2010. New indices and calibrations derived from
432 the distribution of crenarchaeal isoprenoid tetraether lipids: Implications for past sea
433 surface temperature reconstructions. *Geochimica et Cosmochimica Acta* 74, 4639–4654.

434 Kitagawa, H., Fukusawa, H., Nakamura, T., Okamura, M., Takemura, K., Hayashida, A.,
435 Yasuda, Y., 1995. AMS ^{14}C dating of varved sediments from Lake Suigetsu, central Japan
436 and atmospheric ^{14}C change during the late Pleistocene. *Radiocarbon* 37, 371– 378.

437 Kitagawa, H., van der Plicht, J., 1998. A 40,000-year varve chronology from Lake Suigetsu,
438 Japan: extension of the radiocarbon curve. *Radiocarbon* 40, 505–516.

439 Kondo, M., 1985. Oceanographic investigations of fishing grounds in the East China Sea and
440 the Yellow Sea—I, Characteristics of the mean temperature and salinity distributions
441 measured at 50 m and near the bottom. *Bulletin of Seikai Region Fishery Research*
442 *Laboratory* 62, 19–55 (in Japanese with English abstract).

443 Kubota, Y., Kimoto, K., Tada, R., Oda, H., Yokoyama, Y., Matsuzaki, H., 2010. Variations of
444 East Asian summer monsoon since the last deglaciation based on Mg/Ca and oxygen
445 isotope of planktic foraminifera in the northern East China Sea. *Paleoceanography* 25,
446 PA4205.

447 Li, B., Jian, Z., Wang, P., 1997. *Pulleniatina obliquiloculata* as a paleoceanographic indicator
448 in the southern Okinawa Trough during the last 20,000 years. *Marine Micropaleontology*
449 32, 59–69.

450 Li, T., Liu, Z., Hall, M.A., Berne, S., Saito, Y., Cang, S., Cheng, Z., 2001. Heinrich event
451 imprints in the Okinawa Trough: evidence from oxygen isotope and planktonic
452 foraminifera. *Palaeogeography, Palaeoclimatology, Palaeoecology* 176, 133–146.

453 Li, G., Sun, X., Liu, Y., Bickert, T., Ma, Y., 2009. Sea surface temperature record from the
454 north of the East China Sea since late Holocene. *Chinese Science Bulletin* 54, 4507–4513.

455 Lin, Y.S., Wei, K.Y., Lin, I.T., Yu, P.S., Chiang, H.W., Chen, C.Y., Shen, C.C., Mii, H.S.,
456 Chen, Y.G., 2006. The Holocene *Pulleniatina* Minimum Event revisited: geochemical and
457 faunal evidence from the Okinawa Trough and upper reaches of the Kuroshio current.
458 *Marine Micropaleontology* 59, 153–170.

459 Lopes dos Santos, R., Prange, M., Castañeda, I.S., Schefuß, E., Mulitza, S., Schulz, M.,
460 Niedermeyer, E.M., Sinninghe Damsté, J.S., Schouten, S., 2010. Glacial–interglacial
461 variability in Atlantic meridional overturning circulation and thermocline adjustments in
462 the tropical North Atlantic. *Earth and Planetary Science Letters* 300, 407–414.

463 Meng, X., Du, D., Liu, Y., Liu, Z., 2002. Molecular biomarker record of paleoceanographic
464 environment in the East China Sea during the last 35000 years. *Science in China (Series D)*
465 45, 184–192.

466 Nakanishi, T., Yamamoto, M., Irino, T., Tada, R., Distributions of glycerol dialkyl glycerol
467 tetraethers, alkenones and polyunsaturated fatty acids in suspended particulate organic
468 matter in the East China Sea. Submitted to *Journal of Oceanography*.

469 Nakanishi, T., Yamamoto, M., Tada, R., Oda, H., Centennial-scale winter monsoon variability
470 in the northern East China Sea during the Holocene. Submitted to Journal of Quaternary
471 Science.

472 Oba, T., Kato, M., Kitazato, H., Koizumi, I., Omura, A., Sakai, T., Takayama, T., 1991.
473 Paleoenvironmental changes in the Japan Sea during the last 85,000 years.
474 *Paleoceanography* 6, 499–518.

475 Schouten, S., Hopmans, E.C., Schefuß, E., Sinninghe Damsté, J.S., 2002. Distributional
476 variations in marine crenarchaeotal membrane lipids: a new tool for reconstructing ancient
477 sea water temperatures? *Earth and Planetary Science Letters* 204, 265–274.

478 Schouten, S., Hugué, C., Hopmans, E.C., Kienhuis, M.V.M., Sinninghe Damsté, J.S., 2007.
479 Analytical methodology for TEX₈₆ paleothermometry by high performance liquid
480 chromatography/atmospheric pressure chemical ionization-mass spectrometry. *Analytical*
481 *Chemistry* 79, 2940–2944.

482 Shieh, Y.-T., Wang, C.-H., Chen, M.-P., Yung, Y.-L., 1997. The last glacial maximum to
483 Holocene environment changes in the southern Okinawa Trough. *Journal of Asian Earth*
484 *Sciences* 15, 3–8.

485 Shintani, T., Yamamoto, M., Chen, M.-T., 2008. Slow warming of the northern South China
486 Sea during the last deglaciation. *Terrestrial, Atmospheric and Oceanic Sciences*, 19,
487 341–346.

488 Shintani, T., Yamamoto, M., Chen, M.T., 2011. Paleoenvironmental changes in the northern
489 South China Sea over the past 28,000 years: a study of TEX₈₆-derived sea surface
490 temperatures and terrestrial biomarkers. *Journal of the Asian Earth Science* 40, 1221–1229.

491 Sun, Y., Oppo, D.W., Xiang, R., Liu, W., Gao, S., 2005. Last deglaciation in the Okinawa
492 Trough: subtropical northwest Pacific link to northern hemisphere and tropical climate.
493 *Paleoceanography* 20, A4005.

494 Tada, R., Irino, T., Koizumi, I., 1999. Land-ocean linkage over orbital and millennial

495 timescales recorded in late Quaternary sediments of the Japan Sea. *Paleoceanography* 14,
496 236–247.

497 Tanaka, Y., 2003. Coccolith fluxes and species assemblages at the shelf edge and in the
498 Okinawa Trough of the East China Sea. *Deep-Sea Research II* 50, 503–511.

499 Uda, M., 1934. Climatological monthly mean oceanic conditions in the Japan, Yellow, and
500 Okhotsk Seas. *Fisheries Experimental Station Report* 5, 191–236 (in Japanese).

501 Ujiie, H., Tanaka, Y., Ono, T., 1991. Late Quaternary paleoceanographic record from the
502 middle Ryukyu Trench slope, Northwest Pacific. *Marine Micropaleontology* 18, 115–128.

503 Ujiie, H., Ujiie, Y., 1999. Late Quaternary course of the Kuroshio Current in the Ryukyu Arc
504 region, northwestern Pacific Ocean. *Marine Micropaleontology* 37, 23–40.

505 Ujiie, Y., Ujiie, H., Taira, A., Nakamura, T., Oguri, K., 2003. Spatial and temporal variability
506 of surface water in the Kuroshio source region, Pacific Ocean, over the past 21,000 years:
507 evidence from planktonic foraminifera. *Marine Micropaleontology* 49, 335–364.

508 Ujiie, Y., Ujiie, H., 2006. Dynamic changes of the surface and intermediate waters in the
509 Ryukyu Arc region during the past ~250,000 years: based on planktonic and benthic
510 foraminiferal analysis of two IMAGES cores. *Fossils* 79, 43–59 (in Japanese with English
511 abstract).

512 Wahyudi, Minagawa, M., 1997. Response of benthic foraminifera to organic carbon
513 accumulation rates in the Okinawa Trough. *Journal of Oceanography* 53, 411–420.

514 Wang, L., Yang, Z., Zhang, R., Fan, D., Zhao, M., Hu, B., 2011. Sea surface temperature
515 records of core ZY2 from the central mud area in the South Yellow Sea during last 6200
516 years and related effect of the Yellow Sea warm current. *Chinese Science Bulletin* 56,
517 1588–1595.

518 Weijers, J.W.H., Schouten, S., Spaargaren, O.C., Sinninghe Damsté, J.S., 2006. Occurrence
519 and distribution of tetraether membrane in soils: Implications for the use of the BIT index
520 and the TEX₈₆ SST proxy. *Organic Geochemistry* 37, 1680–1693.

521 Xie, S.-P., Hafner, J., Tanimoto, Y., Liu, W.T., Tokinaga, H., Xu, H., 2002. Bathymetric
522 effect on the winter sea surface temperature and climate of the Yellow and East China Seas.
523 *Geophysical Research Letters* 29, 2228.

524 Xu, X., Oda, M., 1999. Surface-water evolution of the eastern East China Sea during the last
525 6,000 years. *Marine Geology* 156, 285–304.

526 Xu, X., Yamasaki, M., Oda, M., Honda, M.C., 2005. Comparison of seasonal flux variations
527 of planktonic foraminifera in sediment traps on both sides of the Ryukyu Islands, Japan,
528 *Marine Micropaleontology* 58, 45–55.

529 Yamamoto, M., Suemune, R., Oba, T., 2005. Equatorward shift of the subarctic boundary in
530 the northwestern Pacific during the last deglaciation. *Geophysical Research Letters* **32**,
531 L05609.

532 Yamamoto, M., 2009. Response of mid-latitude North Pacific surface temperatures to orbital
533 forcing and linkage to the East Asian summer monsoon and tropical ocean-atmosphere
534 interactions. *Journal of Quaternary Science* 24, 836-847.

535 Yamamoto, M., Polyak, L., 2009. Changes in terrestrial organic matter input to the Mendeleev
536 Ridge, western Arctic Ocean, during the Late Quaternary. *Global and Planetary Change* 68,
537 30–37.

538 Yamamoto, M., Shimamoto, A., Fukuhara, T., Tanaka, Y., Ishizaka, J., 2012. Glycerol dialkyl
539 glycerol tetraethers and the TEX₈₆ index in sinking particles in the western North Pacific.
540 *Organic Geochemistry*, <http://dx.doi.org/10.1016/j.orggeochem.2012.04.010>.

541 Yu, H., Xiong, Y., Liu, Z., Berné, S., Huang, C.-Y., Jia, G., 2008. Evidence for the 8,200 a
542 B.P. cooling event in the middle Okinawa Trough. *Geo-Marine Letters* 28, 131–136.

543 Zhang, S.W., Wang, Q.A., Lu, Y., Cui, H., Yuan, Y.L., 2008. Observation of the seasonal
544 evolution of the Yellow Sea Cold Water Mass in 1996–1998. *Continental Shelf Research*
545 28, 442–457.

546 Zhao, M., Huang, C.-Y., Wei, K.-Y., 2005. A 28,000 year U₃₇^{K'} sea surface temperature record

547 of ODP Site 1202B, the southern Okinawa Trough. TAO 16, 45–56.

548 Zhou, H., Li, T., Jia, G., Zhu, Z., Chi, B., Cao, Q., Sun, R., Peng, P., 2007. Sea surface
549 temperature reconstruction for the middle Okinawa Trough during the last
550 glacial-interglacial cycle using C₃₇ unsaturated alkenones. *Palaeogeography,*
551 *Palaeoclimatology, Palaeoecology* 246, 440–453.

552 Zhu, C., Weijers, J.W.H., Wagner, T., Pan, J.-M., Chen, J.-F., Pancost, R.D., 2011. Sources
553 and distributions of tetraether lipids in surface sediments across a large river-dominated
554 continental margin. *Organic Geochemistry* 42, 376–386.

555

556 Figure captions

557

558 Fig. 1. (a) MD98-2195 core location, (b and c) the distribution of seasonal mean winter and
559 summer temperatures at 50 m depth, and the surface water circulation pattern in the East
560 China Sea and the Yellow Sea (Kondo, 1985). KSW = Kuroshio Water. CDW = Changjiang
561 Diluted Water. CCW = Chinese Coastal Water. YSCCW = Yellow Sea Central Cold Water.
562 KBCWK = Kuroshio branch current west of Kyushu. TSWC = Tsushima Warm Current.

563

564 Fig. 2. Seasonal and monthly mean water temperatures at different depths at the study site
565 (Japan Oceanographic Data Center; <http://www.jodc.go.jp/index.html>). “J” to “D” denote the
566 months from January to December. After Nakanishi et al., submitted to Journal of Quaternary
567 Science.

568

569 Fig. 3. Age depth model of core MD98-2195 (Ijiri et al., 2005).

570

571 Fig. 4. Variations in TEX_{86} , TEX_{86}^H , and TEX_{86}^L -derived thermocline temperature, $U_{37}^{K'}$
572 -derived SST (Ijiri et al., 2005), and *Globigerinoides ruber* Mg/Ca-derived SST (Kubota et al.,
573 2010) for the last 42 kyr from core MD98-2195. H0 = the Younger Dryas period, H1 = the
574 Oldest Dryas period. H2 = Heinrich event 2. H3 = Heinrich event 3. H4 = Heinrich event 4.

575

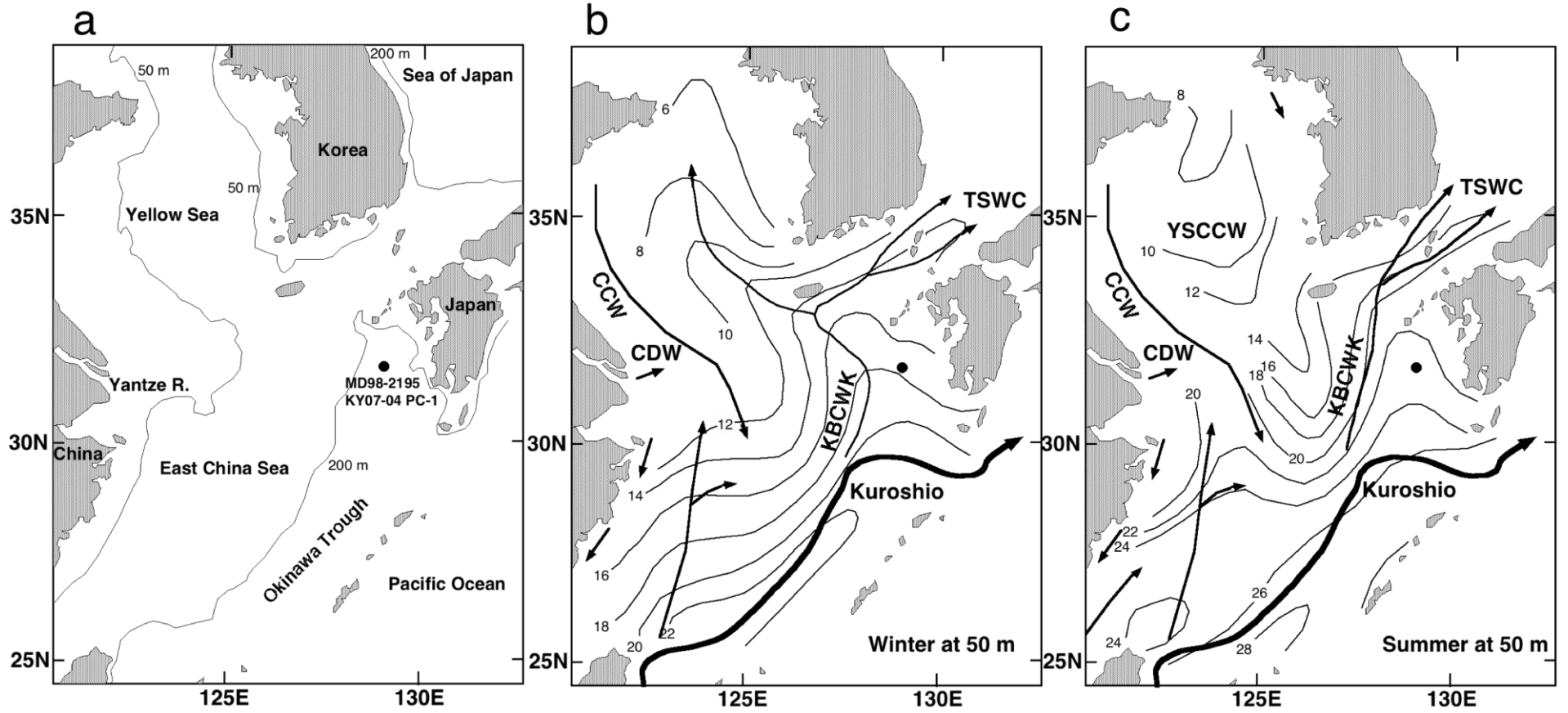
576 Fig. 5. Variation in branched and isoprenoid tetraethers (BIT) index for the last 42 kyr from
577 core MD98-2195.

578

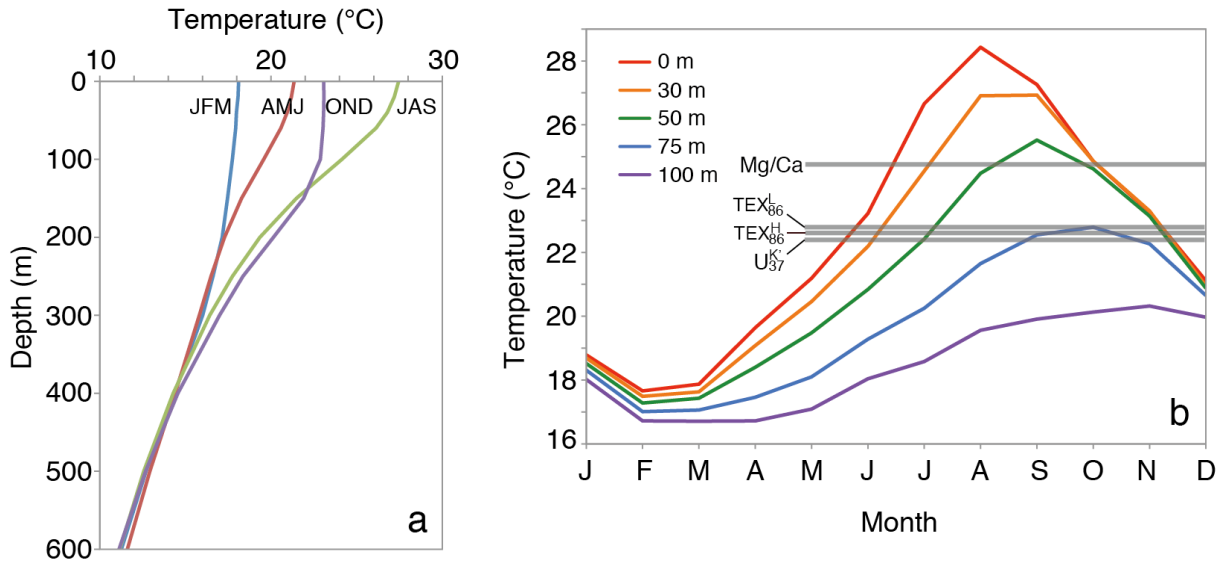
579 Fig. 6. Schematic map showing the distributions of coastline and shallow shelf area in the East
580 China Sea at 15 ka. The sea level was 100 m lower than the present. The cold water was
581 presumably formed near the study site and expanded to the northern Okinawa Trough.

582

583

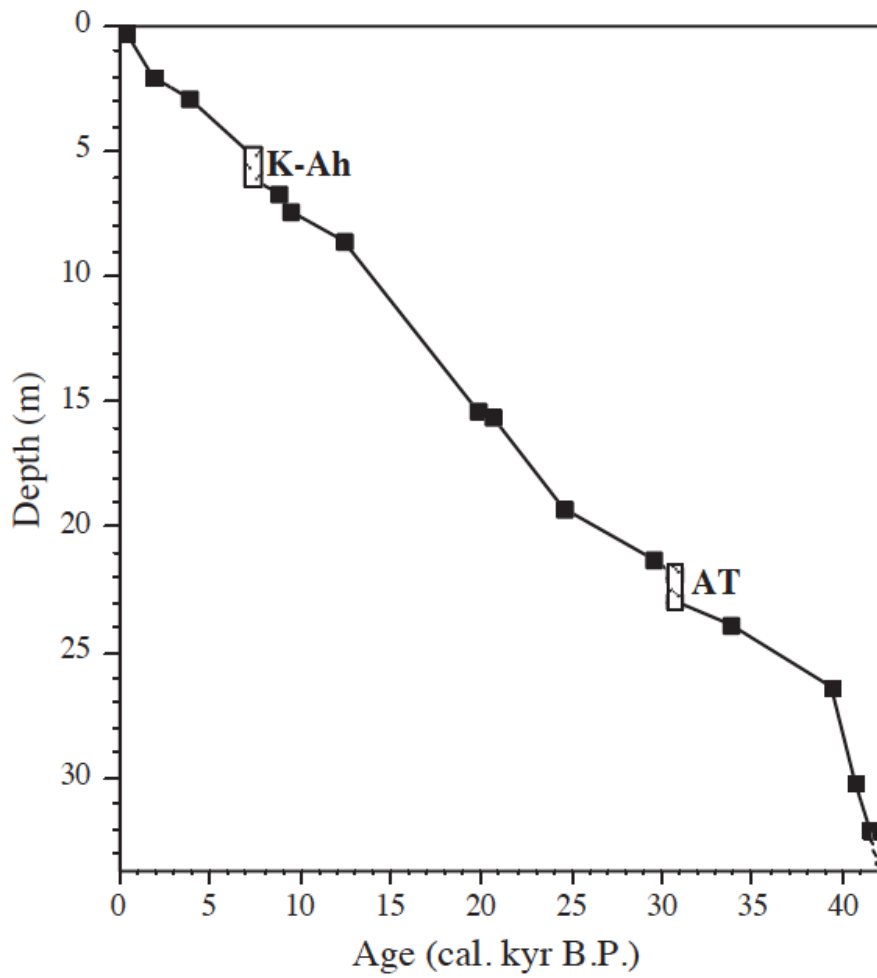


585 Fig. 1.



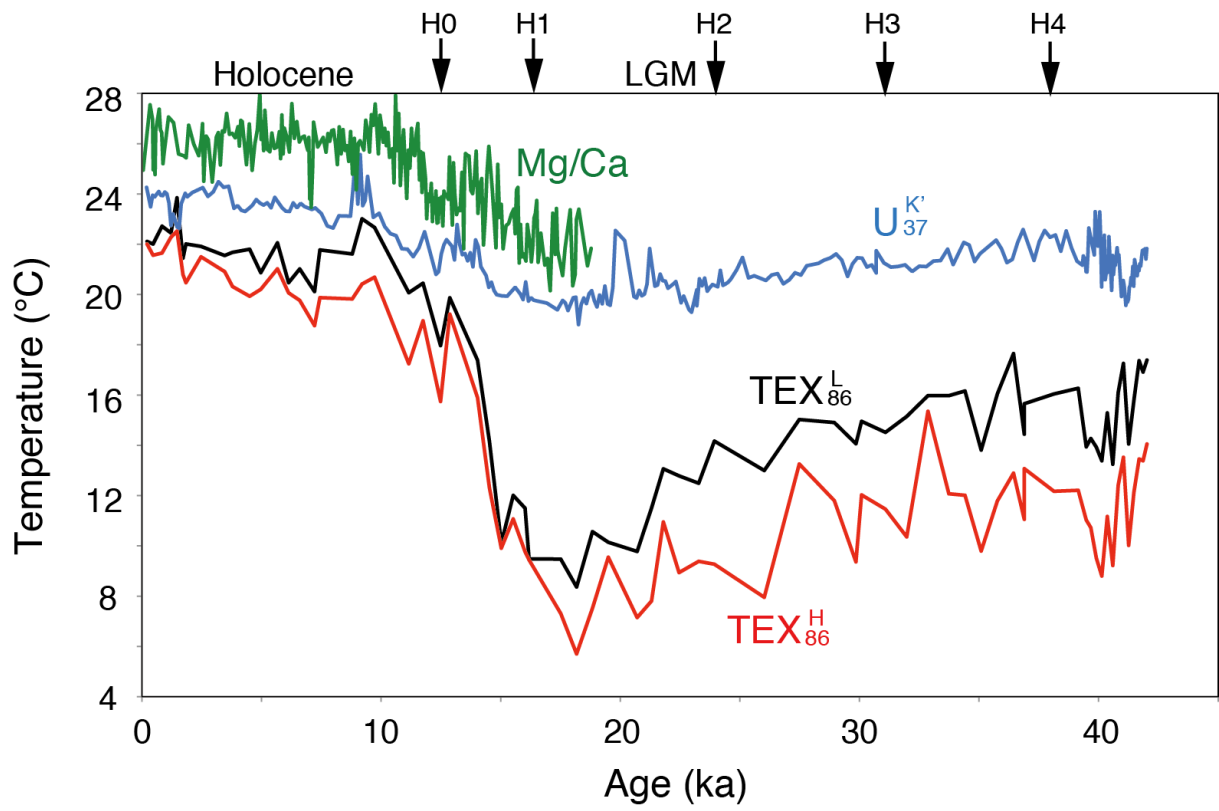
586

587 Fig. 2.



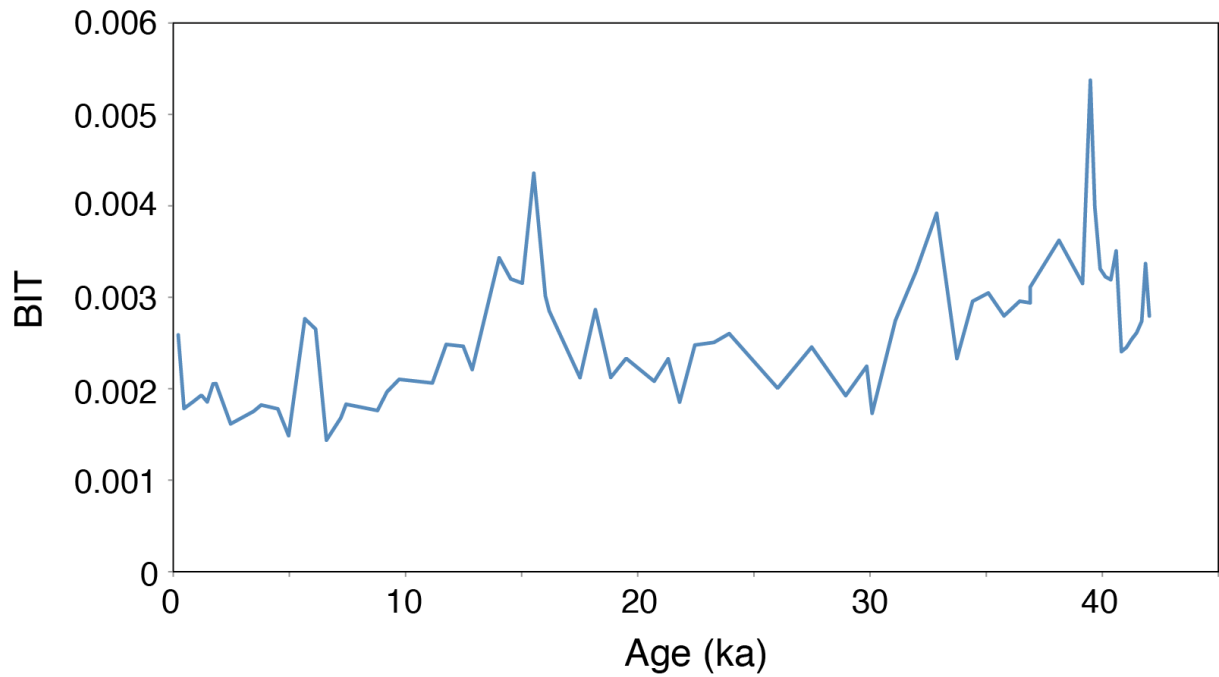
588

589 Fig. 3.



590

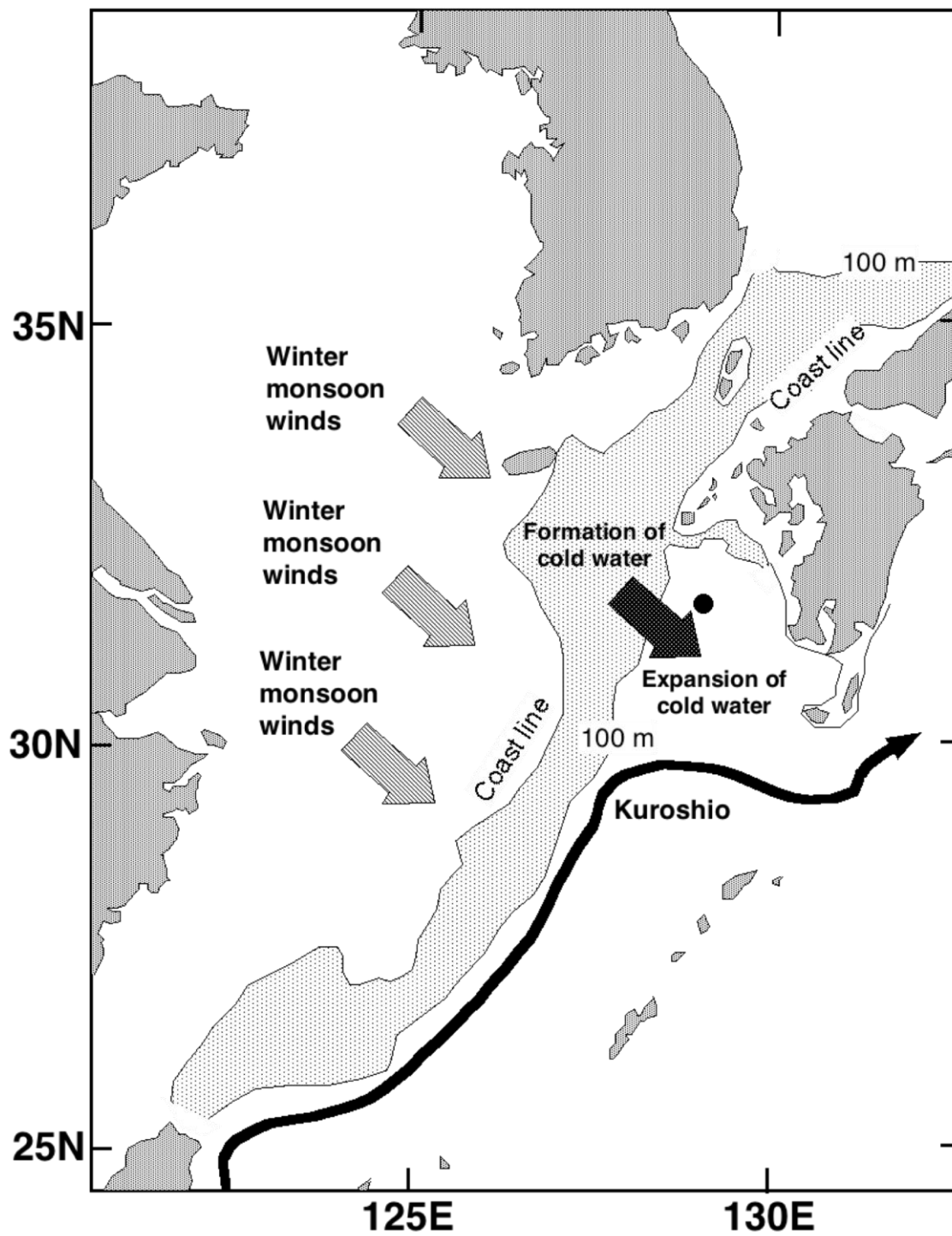
591 Fig. 4.



592

593 Fig. 5.

594



595

596 Fig. 6